Published in "Physical Review B 75: 134413, 2007"
which should be cited to refer to this work.

Relation between directed polymers in random media and random-bond dimer models

Ying Jiang[1] and Thorsten Emig[2]
[1]*Department de Physique, Université de Fribourg, Chemin du Musée 3, CH-1700 Fribourg, Switzerland*
[2]*Laboratoire de Physique Théorique et Modèles Statistiques, CNRS UMR 8626, Université Paris-Sud, 91405 Orsay, France*

We reassess the relation between classical lattice dimer models and the continuum elastic description of a lattice of fluctuating polymers. In the absence of randomness, we determine the density and line tension of the polymers in terms of the bond weights of hard-core dimers on the square and the honeycomb lattice. For the latter, we demonstrate the equivalence of the set of complete dimer coverings and the grand-canonical description of polymers by performing explicitly the continuum limit. Using this equivalence for the random-bond dimer model on a square lattice, we resolve a previously observed discrepancy between numerical results for the random dimer model and a replica approach for polymers in random media. Further potential applications of the equivalence are briefly discussed.

PACS number(s): 75.10.Nr, 05.50.+q, 05.20.−y

I. INTRODUCTION

Dimer coverings of different lattice types have been employed recently as a starting point to study more complex physical systems such as quantum dimer models,[1,2] geometrically frustrated Ising magnets with simple quantum dynamics induced by a transverse magnetic field,[3,4] and elastic strings pinned by quenched disorder.[5,6] The common concept of these approaches is to add to a classical dimer model with a hard-core interaction a perturbation in form of simple quantum dynamics, quenched disorder (random bonds), or additional (classical) dimer interactions. For bipartite lattices, there exists a representation of the dimer model in terms of a height profile of a two-dimensional surface.[7,8] When a fixed height profile with maximally allowed constant tilt is subtracted from the original height profile, one obtains a tilted height profile with terraces of equal height. The steps which separate these terraces form a lattice of directed and noncrossing polymers.[6] Although the height and the polymer representations of dimer models are, on a microscopic level, equivalent descriptions of all dimer states, they allow for different physical interpretations. In the height profile approach, the theory[7] considers Gaussian fluctuations of a coarse-grained height field and, according to its construction, favors states with small tilts, i.e., states with small winding number. In contrast, the polymer description employed in this paper [see Eq. (3) below] is more suitable in the opposite limit where tilted states are actually favored. This can be seen by considering a small polymer density which implies broad terraces in the height profile resulting from the superposition with a fixed maximally tilted reference profile. By construction, across these terraces the original height profile has maximal tilt and hence is strongly tilted if the polymer density is small. It depends on the physical situation described by the dimer model which representation is more useful.

The polymer description has been shown to be a particularly useful physical picture in understanding the effect of quantum fluctuations for an Ising antiferromagnet on a triangular lattice in a transverse field.[3,4,9] Moreover, whereas the "clean" dimer models can be exactly solved on the lattice by Pfaffian methods[10,11] or by free fermion lattice field theories,[12] dimer models with quenched bond disorder are much more difficult to study. Existing studies of lattice dimer models with random-bond weights are all based on numerical approaches. However, a $(1+1)$-dimensional continuum polymer lattice with uncorrelated Gaussian distributed point disorder is one of the very few systems containing quenched randomness and interactions that can be investigated by "exact" methods such as replica theory in combination with Bethe *Ansatz*.[13,14] It is important to check the validity of this approach which involves some assumptions related to the analytic continuation in the replica number and an interchange of the thermodynamic and the zero replica number limit. Since powerful numerical approaches have been employed to study random dimer models, the polymer representation of dimer models provides an independent test of the replica theory. To enable a reliable comparison of the lattice dimer model and the continuum replica theory for polymers, it is important to formulate a continuum description of lattice polymers resulting from the dimer model and to relate the parameters of the two models.

Here, we show that the set of complete dimer coverings maps to the *grand*-canonical ensemble of the polymer system. Regarding the polymers as imaginary-time world lines of free fermions in one dimension, we give a simple derivation of the continuum free energy of the polymers, which agrees with the exact result for dimers if the continuum limit is taken in the way we define it below. Applying the relation between dimers and polymers to the dimer model with random-bond energies, we resolve a previously observed discrepancy between numerical simulations of the dimer system and a replica theory for polymers. We analyze which quantities of the pinned polymers can be probed by simulations of the random dimer model. More specifically, we study the dimer model both on the honeycomb and the square lattice, and discuss the meaning of the different lattice symmetries for the polymer representation. In the presence of bond disorder, we focus on the square lattice since its polymer density is conserved independently of the disorder configuration, and hence shows no sample-to-sample variations. Our results should provide a starting point for other situations where no

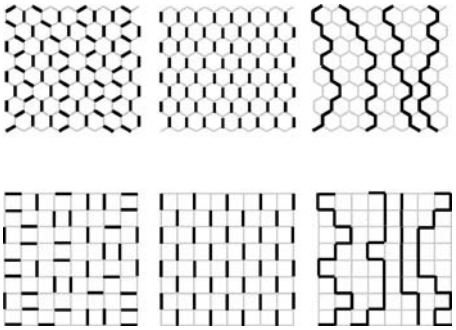

FIG. 1. Mapping of dimer configurations to directed polymers by superposition with a fixed reference covering (middle).

exact solution of the dimer model is possible as, e.g., in a recently studied case of nearest-neighbor dimer interactions.[15] The analogy between directed polymers in two dimensions and Luttinger liquids could be applied to understand more general interacting dimer models.

The rest of the paper is organized as follows. In Sec. II, the relation between the dimer model on the square and the honeycomb lattice and noncrossing directed polymers is reviewed. For the clean case, the continuum limit is defined and the free-energy density of the dimer model and of the polymer model is compared in Sec. III. It is shown that the set of complete dimer coverings is equivalent to the grand-canonical ensemble of polymers. In Sec. IV, the random-bond dimer model is investigated in detail and a previously observed discrepancy between numerical results for the dimer model and the replica theory for pinned polymers is resolved.

II. MODELS: DIMERS AND POLYMERS

The partition function of the dimer model on the honeycomb lattice is given by

$$Z_{\hexagon} = \sum_{\{D\}} z_1^{n_1} z_2^{n_2}, \tag{1}$$

where the sum runs over all complete hard-core dimer coverings of the lattice, and n_1 and n_2 are the numbers of dimers occupying the two types of nonvertical bonds of the honeycomb lattice (see Fig. 1), which carry weights z_1 and z_2, respectively. The weights on the vertical bonds are assumed to be unity. Using the same notation, we define for the square lattice the partition function as

$$Z_{\square} = \sum_{\{D\}} z_1^{n_1}, \tag{2}$$

where n_1 is now the number of dimers covering horizontal bonds which have a weight of z_1, while all vertical bonds carry unity as weight. For these clean dimer models, the partition function and correlation functions are known from exact results.[10,11] For random weights, only numerical results are available (see, e.g., Refs. 5 and 6). However, there is a useful connection between the dimer models and noncrossing directed polymers in (1+1) dimensions. This relation is independent of the actual bond energies, and hence applies also to *random* dimer models. This is particularly interesting since the random-bond energies translate to a pinning potential for the polymers, a problem whose continuum version can be studied in (1+1) dimensions by a replica Bethe *Ansatz*.[13,14] Numerical algorithms for the random dimer model hence provide a unique opportunity to probe the replica symmetric theory which is commonly used to describe pinning of elastic media.

The relation between dimers and polymers is established by superposing every dimer configuration by a fixed reference dimer configuration. For the honeycomb lattice, the reference state consists of a covering of all vertical bonds, whereas for the square lattice a staggered covering of the vertical bonds is chosen (see Fig. 1). In the superposition state, a bond is covered by a dimer (or polymer segment) if it is covered either only in the original state or only in the reference state. Because of the hard-core constraints for the dimers, the polymers are noncrossing. In addition, they are oriented along the vertical direction due to the choice of the reference state.

The same mapping between dimers and polymers on the honeycomb lattice has been used in a recent work.[16] The latter study considers sectors with fixed polymer number. It is easy to verify that all complete dimer coverings can be grouped into sectors specified by the number of polymers or, equivalently, by the number of nonoccupied vertical bonds in a horizontal row of the dimer model. The configurations within a given sector can be transformed into each other by "flipping" those hexagons which have exactly one bond of each of the three bond directions occupied by a dimer. Flipping means that the three dimers are rotated simultaneously by 60°. This transformation obviously does not change the number of polymers but induces a polymer displacement. In this work, we will consider for the honeycomb lattice a superposition of all sectors, resulting in the grand-canonical ensemble of polymers with fluctuating polymer density. The mean polymer density is determined by the weighting of the sectors and hence can be tuned by changing z_1 and z_2. The square lattice, while qualitatively similar to the honeycomb lattice with respect to the usual height representation, does not allow for a tuning of the mean polymer density; it is fixed at $1/2$ independent of z_1 (see below). While for honeycomb lattice a low polymer density corresponds to a strongly tilted height profile, for the square lattice with two different bond weights the height profile cannot acquire different mean tilts. In this sense, the honeycomb and the square lattice are qualitatively different, which becomes obvious in the polymer representation.

The lattice of polymers can be described in the *continuum* limit by an elastic theory which is of the form[5]

$$H_{\mathrm{el}} = \int d^2\mathbf{r} \left\{ \frac{c_{11}}{2}(\partial_x u)^2 + \frac{c_{44}}{2}(\partial_y u)^2 + \rho(\mathbf{r}) V(\mathbf{r}) \right\}, \tag{3}$$

with compression modulus c_{11}, tilt modulus c_{44}, and local polymer density $\rho(\mathbf{r}) = \Sigma_j \delta(x - x_j(y))$, where $x_j(y)$ is the path of the jth polymer. Here, u denotes the continuous displacement field of the polymers so that polymer positions are $x_j(y) = j/\rho + u(j/\rho, y)$ with ρ the mean polymer density. The

random-bond energies are accounted for by a random pinning potential $V(\mathbf{r})$ which is uncorrelated, i.e.,

$$\overline{V(\mathbf{r})V(\mathbf{r}')} = \Delta\,\delta(\mathbf{r}-\mathbf{r}'), \tag{4}$$

so that Δ measures the strength of disorder. In order to compare results for the dimer and the polymer model, we establish a relation between the dimer weights and the elastic constants and the mean density of the polymers. Let us first consider the clean limit with $\Delta \equiv 0$. It is obvious from the mapping between dimers and polymers that the polymer density can vary with the dimer covering. For example, if the dimer state matches exactly the reference state, the polymer density is zero. However, one can define a *mean* polymer density by averaging over all dimer coverings.

For the honeycomb lattice, the mean density is determined by the mean number of occupied nonvertical bonds in the original dimer configuration so that $\rho_{\hexagon}=\langle n_1+n_2\rangle/(\sqrt{3}b_{\hexagon}N)$, where N is the total number of dimers, $b_{\hexagon}$ is the lattice constant, and $\langle\cdots\rangle$ denotes here an ensemble average over all complete dimer coverings. This yields[9,17]

$$\rho_{\hexagon} = \frac{2}{\pi\sqrt{3}b_{\hexagon}} \arcsin\left[\frac{(z_1+z_2)^2-1}{4z_1z_2}\right]^{1/2} \tag{5}$$

if $z_1+z_2>1$ and $\rho_{\hexagon}=0$ if $z_1+z_2\leqslant 1$. For the square lattice, the mean number of polymers is determined by the probability that a vertical bond is occupied by a segment of the polymer. This is the case if the bond is *covered* by a dimer in the original dimer configuration and *not covered* in the reference state, or in the other way around. The probability that a vertical bond is covered by a dimer in the original covering is $p_d=1/2-\phi(z_1)$ with $\phi(z_1)=\arctan(z_1)/\pi$. For the reference state, it is simply $p_r=1/2$. Hence, after the superposition of the two dimer states, the probability that a vertical bond is covered by a polymer is given by $p_d(1-p_r)+p_r(1-p_d)=1/2$ independent of z_1. This fixes the mean density at[5]

$$\rho_{\square} = \frac{1}{2b_{\square}}, \tag{6}$$

where $b_{\square}$ is the lattice constant. Notice that the density on the square lattice does not change with the bond weight z_1.

The elastic constants are length scale dependent due to renormalization effects from the noncrossing constraint. Since there is no additional interaction between the dimers other than the hard-core repulsion, the compression modulus c_{11} is zero on microscopic scales. A finite macroscopic c_{11} is generated by a reduction of entropy due to polymer collisions (see below). The tilt modulus $c_{44}=g\rho$ on microscopic scales (or at very low density) is given by the line tension g of a single polymer and the mean polymer density. The reduced line tension g/T of an individual polymer at temperature T can be obtained from a simple random walk on the lattice,[9] which performs transverse steps according to the weights of the dimer model. For the honeycomb lattice, it reads[9]

$$\frac{g_{\hexagon}}{T} = \frac{2+\eta+1/\eta}{2b_{\hexagon}}, \tag{7}$$

with $\eta=z_1/z_2$, and for the square lattice one has

$$\frac{g_{\square}}{T} = \frac{2z_1+1}{2z_1b_{\square}}. \tag{8}$$

From this result, we see that the polymers become stiffer if one decreases the weights on (one type of) the nonvertical bonds, hence preventing transverse wandering.

III. CLEAN SYSTEM: CONTINUUM LIMIT AND THERMODYNAMIC ENSEMBLES

Before treating the random system, let us first compare the free-energy density of the dimer models and the corresponding polymer lattice by taking the continuum limit. It is important to note that the definition of the continuum limit as given below is distinct from the usual continuum description obtained for the height representation of dimer models from coarse graining. Here, we use the notion "continuum limit" in a natural form where it describes the transition from a lattice model to a continuum model by simultaneously sending the lattice constant to zero and decreasing the lattice polymer density so that the continuum polymer density remains constant. We first note that the free energy of the dimer model on the honeycomb lattice can be computed exactly.[17] By changing variables from z_1, z_2 to $\eta=z_1/z_2$ and $\rho_{\hexagon}$, one can express the free-energy density in terms of the physical quantities of the polymers on the lattice.[9] The result is

$$f_{\mathrm{dimer}} = -\frac{2\pi}{\sqrt{3}}\int_0^{\rho_{\hexagon}} d\rho' \frac{\eta\rho'\,\sin(\pi\sqrt{3}b_{\hexagon}\rho')}{1+\eta^2+2\eta\cos(\pi\sqrt{3}b_{\hexagon}\rho')}, \tag{9}$$

where the energy is measured relative to the line $z_1+z_2=1$ at which a Kasteleyn transition to a phase with vanishing lattice polymer density occurs. We perform the continuum limit explicitly by sending $b_{\hexagon}\to 0$ while keeping the line tension $b_{\hexagon}g_{\hexagon}/T$ and the continuum polymer density $\rho_{\hexagon}$ fixed. This can be achieved by adjusting the bond weights z_1 and z_2 so that the Kasteleyn transition at $z_1+z_2=1_+$ is approached from above along the direction with constant $\eta=z_1/z_2$. Physically, this limit means for the dimer lattice model that the energy on the nonvertical bonds is increased so that it becomes more favorable to occupy more vertical bonds by dimers. The superposition procedure shown in Fig. 1 then leads to a *reduction* of occupied vertical bonds for the corresponding polymer configuration, and hence the lattice polymer density tends to zero. Since the lattice constant $b_{\hexagon}$ is sent to zero simultaneously, a fixed number of polymers per continuum area is maintained.

This definition of the continuum limit yields the free-energy density for the continuum version of the dimer model, expressed in terms of the polymer parameters,

$$f_{\mathrm{dimer}} = -\frac{\pi^2}{3}\frac{T}{g_{\hexagon}}\rho_{\hexagon}^3, \tag{10}$$

where we used Eq. (7).

An alternative approach to treat a system of interacting polymers in (1+1) dimensions is to regard each polymer as a world line of a fermion in imaginary time. Then, the noncrossing constraint is naturally guaranteed by the Pauli principle. If the length L_y of the polymers tends to infinity, their *reduced* free energy $L_y E_0/\hbar$ is given by the ground-state energy $E_0=(\pi^2/6)(\hbar^2/m)\rho^3 L_x$ of one-dimensional fermions at density ρ. Using the mapping $m\to g$ and $\hbar\to T$, one gets for the reduced free-energy density of the polymers at fixed density

$$f_{\rm poly}=\frac{\pi^2}{6}\frac{T}{g}\rho^3. \tag{11}$$

Although the scaling of this result with the physical parameters is the same as for the free energy in the continuum limit of the dimer model [Eq. (10)], the amplitudes do not agree. However, as we discussed in the preceding section, while each sector of dimer configurations corresponds to a fixed number of polymers, when considering the total set of dimer configurations the number of polymers is no longer fixed. Hence, we have to compare the dimer free energy with the potential of the grand-canonical ensemble of the polymers. The chemical potential is obtained as $\mu=\partial f_{\rm poly}/\partial\rho=(\pi^2/2)\times(T/g)\rho^2$, yielding the grand-canonical potential density

$$j_{\rm poly}=f_{\rm poly}-\mu\rho=-\frac{\pi^2}{3}\frac{T}{g}\rho^3, \tag{12}$$

which is in full agreement with the continuum limit of the exact solution of the dimer model of Eq. (10). This demonstrates that dimer model can be described on large length scales as free fermions where their mass is determined in terms of the bond weights by a random walk of a single polymer on the lattice.

It is instructive to compare the exact lattice result for the dimer free energy of Eq. (9) and the potential $j_{\rm poly}$ with $g_{\hexagon}$ of Eq. (7) even for larger $b_{\hexagon}\rho_{\hexagon}$. By numerical integration of Eq. (9), we obtain the ratio $f_{\rm dimer}/j_{\rm poly}$ over the entire range of possible polymer densities shown in Fig. 2. Up to approximately 1/4 of the maximal density, we find reasonable agreement between the lattice and continuum results, almost independent of the anisotropy $\eta=z_1/z_2$. For larger densities, the value of η becomes important. There is an optimal value of η close to 1/3 for which the continuum description gives accurate results (within a few percent) even for all densities.

The anisotropy of the dimer model can be tuned by changing the relative magnitude of the weights z_1 and z_2. The exact solution of the dimer model on the honeycomb lattice yields for the correlation lengths the result[17]

$$\xi_x=\frac{\sqrt{3}b_{\hexagon}}{2\phi_0}=\frac{1}{\pi\rho_{\hexagon}},\quad \xi_y=\frac{3b_{\hexagon}}{4z_1z_2\phi_0\sin 2\phi_0}, \tag{13}$$

with $\phi_0=\arcsin\sqrt{[(z_1+z_2)^2-1]/(4z_1z_2)}$. Hence, the correlation length perpendicular to the direction of the polymers is set by their mean distance $1/\rho_{\hexagon}$. The length ξ_y should then be set by the typical scale a polymer can wander freely before it reaches a transverse displacement of the order of the mean distance between polymers. In the continuum description of the polymers, the random-walk description of a single polymer then implies the relation

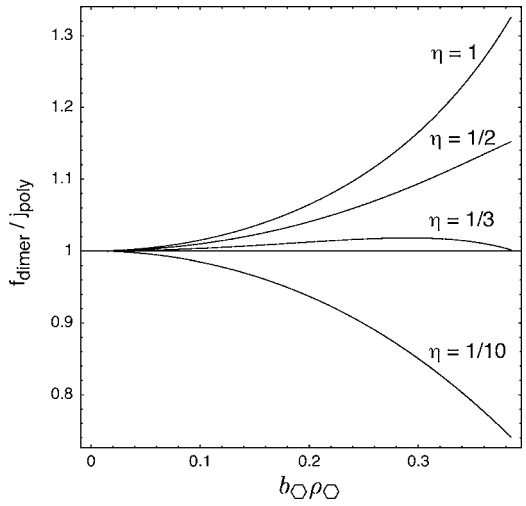

FIG. 2. Comparison of the free energy $f_{\rm dimer}$ of the honeycomb lattice dimer model [Eq. (9)] and the grand-canonical potential $j_{\rm poly}$ of the continuum polymer system [Eq. (12)] with the expression of Eq. (7) for g/T substituted. The curves extend to $\rho_{\hexagon}=2/(3^{3/2}b_{\hexagon})$, which is the maximal polymer density on the lattice for $\eta=1$. However, in the lattice model, the density cannot become larger than $\rho_{\hexagon}=2/(\pi\sqrt{3})\arcsin(\sqrt{2+\eta}/2)$ by tuning the weights at a fixed ratio η.

$$\xi_x^2=\frac{T}{g_{\hexagon}}\xi_y \tag{14}$$

between the correlation lengths. Together with the first relation of Eq. (13), this yields the anisotropy

$$\frac{\xi_x}{\xi_y}=\pi\frac{T}{g_{\hexagon}}\rho_{\hexagon}. \tag{15}$$

That this result is consistent with the anisotropy of the elastic description of the polymer system follows from the macroscopic compression modulus which is given by the compressibility, i.e., $c_{11}=T\rho^2\partial^2 f_{\rm poly}/\partial\rho^2$ in terms of the reduced free energy of Eq. (11). This yields $c_{11}=\pi^2(T^2/g)\rho^3$ and hence together with $c_{44}=g\rho$

$$\frac{\xi_x}{\xi_y}=\sqrt{\frac{c_{11}}{c_{44}}}. \tag{16}$$

In order to connect the lattice and continuum descriptions further, one would like to know under what conditions the lattice correlation lengths of Eq. (13) fulfill the continuum relation of Eq. (14). To address this question, we change again variables from z_1, z_2 to $\eta=z_1/z_2$ and $\rho_{\hexagon}$. If one uses the result for $g_{\hexagon}$ of Eq. (7), one can easily check that Eq. (14) is indeed fulfilled in the continuum limit $b_{\hexagon}\to 0$. The convergence of the anisotropy of the dimer model to that of the continuum description in terms of polymers is shown in Fig. 3 for different η. Hence, the exact anisotropy factor $\sqrt{c_{11}/c_{44}}$ of the continuum elastic model is recovered. This is important if one compares free-energy *densities* of systems with different anisotropies since then the ratio of system sizes

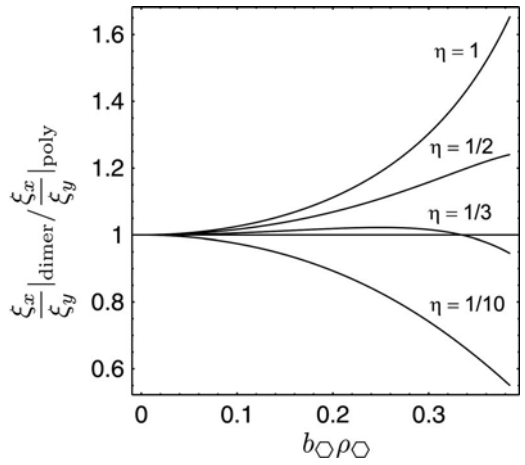

FIG. 3. Comparison of the anisotropy $\xi_x/\xi_y|_{\text{dimer}}$ of the lattice dimer model, taken from Eq. (13), and the anisotropy $\xi_x/\xi_y|_{\text{poly}}$ of the continuum polymer system, Eq. (15).

must be chosen as to match the ratio of their anisotropies.

For the dimer model on the square lattice, there is no direct analog of the previous analysis since the mean polymer density cannot be tuned by changing the weight z_1 but is fixed [see Eq. (6)]. Hence, one cannot take the continuum limit explicitly. Nevertheless, the square lattice is particularly useful if one wants to study the effect of random bonds since the polymer density is robust against variations of the weights and thus shows no disorder induced fluctuations. For the clean square lattice dimer model, we can use the insight we gained from the previous analysis of the honeycomb lattice to compare the free energies of the square lattice and the continuum model. The exact reduced free-energy density of the lattice model is known to be[10]

$$f_{\text{dimer}} = -\frac{1}{\pi b_\square^2}\int_0^{z_1} dv \frac{\arctan v}{v}. \tag{17}$$

The continuum free fermion result of Eq. (12) yields, in combination with the random-walk result of Eq. (8) for the line tension on the square lattice, the estimate for the reduced free-energy density,

$$f_{\text{dimer}} = -\frac{\pi^2}{3}\frac{z_1 b_\square}{z_1 + 1/2}\rho_\square^3. \tag{18}$$

Below, we will study the square lattice with bond energies that are randomly distributed with mean zero so that the clean limit corresponds to the isotropic case $z_1=1$. For this case, Eq. (17) yields the exact result $f_{\text{dimer}} b_\square^2 = -G/\pi = -0.2916$, which is close to the continuum approximation of Eq. (18) which predicts $f_{\text{dimer}} b_\square^2 = -\pi^2/36 = -0.2742$ at the fixed density $\rho_\square = 1/(2b_\square)$.

IV. RANDOM BONDS AND PINNED POLYMERS

In this section, we will consider exclusively the square lattice but with random energies ϵ_{ij} assigned to all vertical bonds so that $z_{ij} = \exp(-\epsilon_{ij}/T_d)$, where z_{ij} now denotes the weight on the bond (ij). The dimer temperature T_d measures the strength of disorder. The energies ϵ_{ij} are drawn for each bond independently from a Gaussian distribution with zero mean and unit variance. On all horizontal bonds, we set $\epsilon_{ij} = 0$ so that for $T_d \to \infty$ the isotropic clean dimer model is recovered. The partition function can be written as

$$Z_\square = \sum_{\{D\}} \exp\left(-\sum_{(ij)\in D} \epsilon_{ij}/T_d\right), \tag{19}$$

where the second sum runs over all occupied bonds. The disorder averaged free energy and correlations of this model have been computed by a polynomial algorithm[18,19] for system sizes up to 512×512 lattice sites and typically 6000 disorder samples.[5,18]

On the analytical side, progress has been made for the polymer system with random pinning by applying the replica method. Regarding again each polymer of the replicated theory as a fermion in imaginary time, and applying the Pauli principle for all particles within the same replica, the replica free energy can be obtained again as the ground-state energy of a one-dimensional system of fermions. Due to the replication, the fermions now carry n spin components and interact via an attractive δ-function potential arising from the short-ranged disorder correlations. This SU(n) Fermi gas can be studied by a series of nested Bethe *Ansätze*.[13] In the limit $n \to 0$, the Bethe *Ansatz* equations can be solved exactly for arbitrary disorder strength Δ, yielding the disordered averaged reduced free-energy density of the polymers,[20]

$$\bar{f}_{\text{poly}} = \bar{f}_0(\Delta)\rho + \frac{\pi^2}{6}\frac{T}{g}\rho^3 + \frac{\Delta}{2T^2}\rho^2, \tag{20}$$

where $\bar{f}_0(\Delta)$ represents the disorder dependent free energy of a single polymer. Notice the simple form of the disorder contribution to the free energy of the pure system [cf. Eq. (11)]. Interestingly, in the limit of strong interactions (disorder), the SU(n) Fermi gas in the limit $n \to 0$ becomes identical to the (pure) interacting Bose gas studied by Lieb and Liniger.[21] Since it was shown that the interaction strength scales as n^2, perturbation theory for the ground-state energy of the Bose gas yields a series expansion in n of the replica free energy for large disorder. The coefficients of this expansion correspond to the disorder averaged cumulants of the free energy, which hence are known exactly from the replica Bethe *Ansatz*.[14]

The prediction of the replica approach can be compared to the numerical evaluation of the free energy and its cumulant averages for the random-bond dimer model. This has been done in Ref. 5, neglecting, however, fluctuations in the polymer density induced by the statistics of the pure dimer model. While nice agreement was found for the second and third cumulants of the free energy, the averaged free energies were only consistent if a term $\sim\Delta^2$ of the single polymer contribution $\bar{f}_0$ was dropped by hand. However, contributions $\sim n^3\Delta^2$ from the replica free energy of a single polymer were found to be crucial for the agreement of the third cumulant of the total free energy. A similar observation was made[5] for the data obtained previously for a single pinned polymer.[22] This is, in particular, unsatisfying due to the model character of the directed polymer in a random potential for the theory of

disordered systems. Below, we show that the differences between the replica approach for polymers and the numerical results on the dimer model can be fully reconciled when polymer density fluctuations are included. As demonstrated for the clean system, this can be done by comparing the set of complete dimer coverings to the grand-canonical ensemble of polymers. It follows from Eq. (20) that the disorder averaged chemical potential $\bar{\mu}=\partial \bar{f}_{\rm poly}/\partial\rho$ since disorder induces no (additional) fluctuations in ρ. Thus, the averaged grand-canonical potential density is

$$\bar{j}_{\rm poly}=-\frac{\pi^2}{3}\frac{T}{g}\rho^3-\frac{\Delta}{2T^2}\rho^2, \tag{21}$$

so that the single polymer term $\bar{f}_0$ cancels. Notice that $\bar{f}_0$ is exactly the term which was in disagreement with numerical results for the random-bond dimer model. Hence, the disorder averaged free energy of a single directed polymer cannot be determined from numerical computations of the free energy of the dimer model. However, it is the disorder induced effective *interaction* of the polymers which determines the dimer free energy. To obtain the latter, we substitute the dimer parameters $\rho=\rho_\square=1/(2b_\square)$ and g/T from Eq. (8) into Eq. (21). The disorder strength Δ/T^2 must be related to the dimer temperature T_d, which measures the variance of the bond energies. As was shown in Ref. 5, the relation is

$$\frac{\Delta}{T^2}=\frac{\xi_d}{b_\square}\frac{1}{T_d^2}, \tag{22}$$

where the length ξ_d acts as a cutoff in the continuum model over which the δ function of Eq. (4) is smeared out. The ratio $\xi_d/b_\square$ must be considered as a fitting parameter which should turn out to be of order unity. As we are comparing energy densities, the disorder dependent anisotropy $\sqrt{c_{11}/c_{44}}$ of the polymer system must be included.[5] This yields for the disorder averaged free-energy density of the dimers

$$\bar{f}_{\rm dimer}=b_\square^2\sqrt{\frac{c_{44}}{c_{11}}}\bar{j}_{\rm poly}. \tag{23}$$

The compression modulus can be obtained again from the (averaged) polymer free energy of Eq. (20), $c_{11}=T\rho^2\partial^2\bar{f}_{\rm poly}/\partial\rho^2$, yielding for the anisotropy

$$\sqrt{\frac{c_{44}}{c_{11}}}=\frac{1}{\pi\rho}\frac{g}{T}\left(1+\frac{g\Delta}{\pi^2T^3\rho}\right)^{-1/2}. \tag{24}$$

In order to correct for a (small) difference between lattice and continuum models, we match with the exact result $f_{\rm dimer}=-G/\pi$ of Eq. (17) with $z_1=1$ in the clean limit $T_d\to\infty$. Then, we obtain in terms of the dimer parameters the final result

$$\bar{f}_{\rm dimer}=-\frac{G+\frac{3}{8}\frac{\xi_d}{b}T_d^{-2}}{\sqrt{\pi^2+3(\xi_d/b)T_d^{-2}}}, \tag{25}$$

which has to be compared to the result for $\overline{\ln Z_l}/L^2=-\bar{f}_{\rm dimer}$ of Eq. (32) in Ref. 5, where the single polymer contributions had been included, resulting in an additional term $\sim T_d^{-4}$ in the numerator of Eq. (25). Exactly, the latter term was found to be in disagreement with simulation data. The expression of Eq. (25) is plotted in Fig. 4 together with the original simulation data for the random dimer model, demonstrating indeed nice agreement for $\xi_d/b_\square=1.33$.

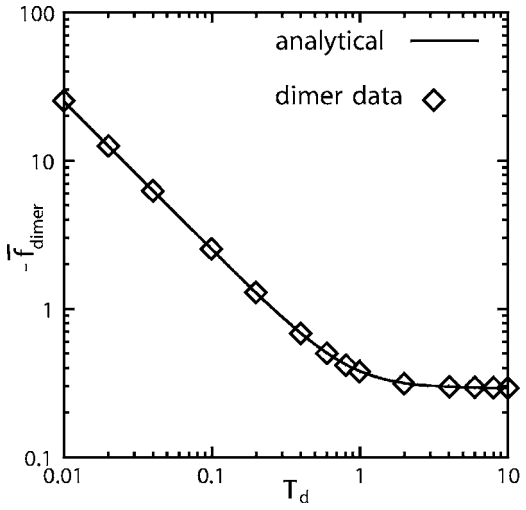

FIG. 4. Disorder averaged free-energy density for the random-bond dimer model [Eq. (25) with $\xi_d/b_\square=1.33$] and corresponding simulation data, taken from Ref. 5.

Finally, we comment on higher cumulant averages of the dimer free energy. They were also measured in simulations and were shown to agree with the free-energy fluctuations of the polymer system.[5] This can be easily understood from the fact that on the square lattice, there are no sample-to-sample variations of the mean polymer density. Hence, the shift of the polymer free energy by $-\mu\rho$ in Eq. (12) is independent of disorder so that one has identical disorder averaged cumulants in the canonical and grand-canonical ensembles, $[j^p]_c=[f^p]_c$ for $p\geq 2$, where $[\cdots]_c$ denotes a cumulant average over disorder. Because of that, *fluctuations* of the single polymer free energy f_0 are important for the dimer model. This explains why contributions $\sim n^3\Delta^2$ from a single polymer to the replica free energy had to be included in Ref. 5 to obtain agreement for the third cumulant of the free energy between polymer and dimer models.

V. OUTLOOK

We have shown that a continuum polymer model can provide a good approximation to dimer models on bipartite lattices. Although the polymer description yields, in general, not the exact result, it provides a more physical picture of the dimer model as its exact solution which, moreover, is available only in the clean limit. Lattice Ising spin models with geometric frustration can exactly be mapped at zero temperature to classical dimer models on the dual lattice.[8] The effect of thermal fluctuations and/or a transverse magnetic field can be understood in terms of topological defects in the polymer representation of the dimer model.[9] Here, we have shown that the influence of random bonds in the dimer model can be described as pinning of polymers. This implies that the glassy state of certain spin models with random couplings

could be related to the glass phase of polymers in a random environment. For example, it can be easily checked that random dilution of the triangular Ising antiferromagnet leads to a pinning of the polymers at the nonmagnetic lattice sites. Another potential application of our results is the study of classical dimers which, in addition to the hard-core repulsion, interact in a more general way. Since the mapping to polymers is independent of the dimer interaction, one can use the analogy between directed polymers and world lines of bosons in imaginary time to explore dimer interactions in terms of interacting bosons in one dimension. Recently, the classical limit (without a kinetic term) of the quantum dimer model on the square lattice has been shown to have a phase transition between a critical and a columnar phase due to the aligning interaction.[15] The correlations in the critical phase are found to decay with an exponent that varies continuously with the interaction amplitude. Using the mapping to world lines of bosons, that exponent is determined by the compressibility of the Bose gas which presumably can be modeled by a tight-binding Hamiltonian with an infinite on-site repulsion and a nearest neighbor interaction.[23]

ACKNOWLEDGMENTS

Y.J. is indebted to D. Baeriswyl for interesting discussions and acknowledges the financial support by Swiss National Science Foundation through Grant No. 200020-105446.

[1] D. S. Rokhsar and S. A. Kivelson, Phys. Rev. Lett. **61**, 2376 (1988).
[2] R. Moessner and S. L. Sondhi, Phys. Rev. Lett. **86**, 1881 (2001); G. Misguich, D. Serban, and V. Pasquier, *ibid.* **89**, 137202 (2002); R. Moessner and S. L. Sondhi, Phys. Rev. B **68**, 184512 (2003).
[3] R. Moessner and S. L. Sondhi, Phys. Rev. B **63**, 224401 (2001).
[4] Y. Jiang and T. Emig, Phys. Rev. Lett. **94**, 110604 (2005).
[5] S. Bogner, T. Emig, A. Taha, and C. Zeng, Phys. Rev. B **69**, 104420 (2004).
[6] C. Zeng, A. A. Middleton, and Y. Shapir, Phys. Rev. Lett. **77**, 3204 (1996).
[7] C. L. Henley, J. Stat. Phys. **89**, 483 (1997).
[8] H. W. J. Blöte and H. J. Hilhorst, J. Phys. A **15**, L631 (1982); B. Nienhuis, H. J. Hilhorst, and H. W. J. Blöte, *ibid.* **17**, 3559 (1984).
[9] Y. Jiang and T. Emig, Phys. Rev. B **73**, 104452 (2005).
[10] P. W. Kasteleyn, Physica (Amsterdam) **27**, 1209 (1961); M. E. Fisher, Phys. Rev. **124**, 1664 (1961); M. E. Fisher and J. Stephenson, *ibid.* **132**, 1411 (1963).
[11] P. W. Kasteleyn, J. Math. Phys. **4**, 287 (1963); M. E. Fisher, *ibid.* **7**, 1776 (1966).
[12] S. Samuel, J. Math. Phys. **21**, 2806 (1980).
[13] M. Kardar, Nucl. Phys. B **290**, 582 (1987).
[14] T. Emig and M. Kardar, Nucl. Phys. B **604**, 479 (2001).
[15] F. Alet, J. L. Jacobsen, G. Misguich, V. Pasquier, F. Mila, and M. Troyer, Phys. Rev. Lett. **94**, 235702 (2005).
[16] A. Dhar, P. Chaudhuri, and C. Dasgupta, Phys. Rev. B **61**, 6227 (2000).
[17] C. S. O. Yokoi, J. F. Nagle, and S. R. Salinas, J. Stat. Phys. **44**, 729 (1986).
[18] C. Zeng, P. L. Leath, and T. Hwa, Phys. Rev. Lett. **83**, 4860 (1999).
[19] N. Elkies, G. Kuperberg, M. Larsen, and J. Propp, J. Algebr. Comb. **1**, 111 (1992); **1**, 219 (1992).
[20] T. Emig and S. Bogner, Phys. Rev. Lett. **90**, 185701 (2003).
[21] E. H. Lieb and W. Liniger, Phys. Rev. **130**, 1605 (1963).
[22] J. Krug, P. Meakin, and T. Halpin-Healy, Phys. Rev. A **45**, 638 (1992).
[23] I. Affleck, W. Hofstetter, D. R. Nelson, and U. Schollwöck, J. Stat. Mech.: Theory Exp. 2004, P10003.